JETP Letters, Vol. 79, No. 9, 2004, pp. 399–401. Translated from Pis'ma v Zhurnal Éksperimental'noĭ i Teoreticheskoĭ Fiziki, Vol. 79, No. 9, 2004, pp. 504–506.

Measurements of X-Ray Absorption Spectra by the Prism Spectroscopy Method

A. G. Tur'yanskii*, I. V. Pirshin, and D. V. Belyanskii

Lebedev Physical Institute, Russian Academy of Sciences, Leninskiĭ pr. 53, Moscow, 119991 Russia

**e-mail: tour@mail1.lebedev.ru*

Received April 1, 2004

X-ray absorption spectra of a number of samples were measured in the range 5–30 keV by the prism spectrophotometry method. The spectral decomposition was performed using an optically polished diamond prism with an opening angle of 90°. The absorption spectra of liquid bromonaphthalene are presented as an example. An energy resolution of 100–130 eV was achieved in the energy range of ~10 keV, providing the unambiguous identification of elements by jumps in the *K* photoabsorption. © *2004 MAIK "Nauka/Interperiodica".*

PACS numbers: 07.85.Nc; 41.50.+h

The possibility of the spectral decomposition of X radiation using a diamond prism has been substantiated in recent works [1–3] and experimentally tested through recording intense X-ray tube emission spectra. It is evident, however, that only the possibility of determining the sample composition from the absorption spectra is a criterion for the practical importance of the suggested method.

In this work, an improved spectrometer scheme is described that provides a manyfold increase in the sensitivity and accuracy. It was used to record the X-ray absorption spectra of a number of samples by the prism spectroscopy method.

It is known that the width of the *K*-absorption jump is $\Delta E_K \sim \Gamma_K$ [4], where Γ_K is the width of an atomic level in the *K* shell (1*s* state). According to [5], Γ_K varies within 0.5–50 eV for the majority of chemical elements. The energy shift ΔE_C caused by the chemical bonding of atoms ordinarily does not exceed 1–4 eV [6, 7]. At the same time, the difference $\Delta E_B = E_K(Z + 1) - E_K(Z)$ in the *K*-electron binding energies of atoms of the neighboring elements in the periodic table is equal to 0.5–2.5 keV for $Z > 20$. That is, $\Delta E_B \gg \Delta E_K$ and $\Delta E_B \gg \Delta E_C$. Thus, measurements of the positions of *K*-absorption jumps with a resolution no worse than $\Delta E_B/2$ allow the practically unambiguous identification of elements entering the sample composition. With minor reservations, this statement can be extended to the *L*-absorption jumps for the elements with $Z > 50$.

The X-ray optical scheme of a prism spectrometer in the measurement plane is shown in Fig. 1. Sharp-focus X-ray tube *1* with a copper anode serves as a radiation source. The sizes of the focus projection onto the plane normal to the analyzed beam are 40 μm in the measurement plane and 8 mm in the perpendicular direction. Two X-ray goniometers *5* and *11* are placed in the beam path. A diamond prism with the opening angle $\alpha = 90°$ between the refracting faces is placed at the axis of the first goniometer. The prism is made from a single crystal of natural diamond. The angle of incidence φ of a primary beam on the prism entrance face was chosen to be ~1 mrad. With these values of α and φ, the radiation passes through the entrance face almost without deflection, so that the beam glancing angle relative to the exit face is $\theta = \varphi$. The advantages of this spectrometric geometry were substantiated in our work [3]. The area of the refracting face is 12 mm^2. The first goniometer is designed for the prism angular tuning against the specular reflection from the refracting face. The tuning is accomplished using detector *10*, ahead of which a monochromator *8* is placed to set off the CuK_α line (0.154 nm). The second goniometer serves for the angular displacement of main detector *13* containing a 1-mm-thick NaI(Tl) crystal and a photomultiplier. This provides a ≥90% efficiency of quantum detection in the energy range $E < 30$ keV.

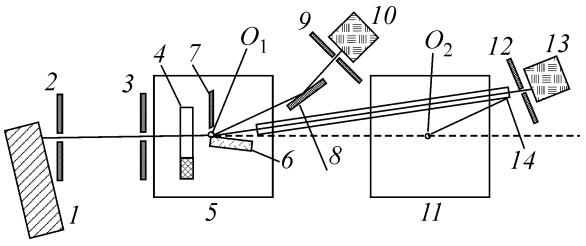

Fig. 1. Scheme of a prism spectrometer: (*1*) X-ray tube; (*2*, *3*) collimator slits; (*4*) sample; (*5*, *11*) goniometers; (*6*) diamond prism; (*7*) absorbing screen; (*8*) monochromator; (*9*, *12*) receiving slits; (*10*, *13*) radiation detectors; (*14*) pumped-out collimator.

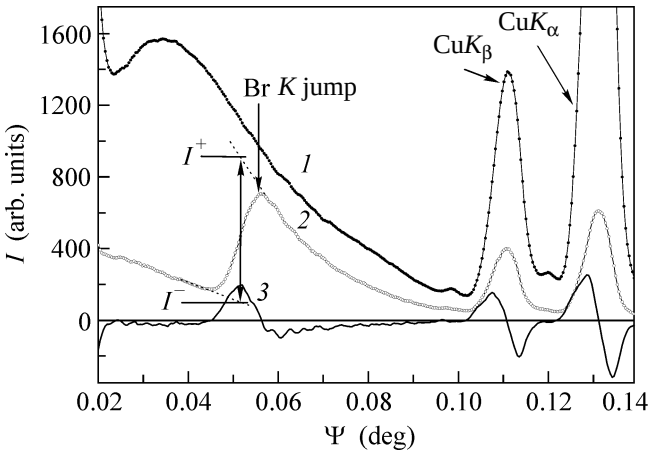

Fig. 2. Angular dependences $I(\Psi)$ of the intensity of refracted radiation: (*1*) before the introduction of a bromonaphthalene ($C_{10}H_7Br$) sample; (*2*) after the introduction; (*3*) $dI/d\Psi$ derivative of curve *2*.

The distances from the X-ray-tube focus to the principal axes O_1 and O_2 of goniometers *5* and *11* are equal to 330 and 1161 mm, respectively, and from the axes O_1 and O_2 to detector slits *9* and *12* are equal to 225 and 192 mm, respectively. Since the spectrum is decomposed on the O_1 axis, while the detector is rotated about the O_2 axis, the scheme provides a factor-of-$(L + R)/R$ = 5.3 increase in the angular resolution for the indicated recording scheme. A sample *4* under study was placed between the collimator exit slit and the diamond prism. To minimize losses caused by the attenuation and scattering of X radiation in air, a vacuum collimator (*14*) 960 mm long with windows made from a 0.2-mm-thick Be foil was placed between the O_1 axis and receiving detector *13*. The collimator provided a more than one order of magnitude increase in the intensity of the detected signal in the energy range $E < 6$ kV. Measurements were made with a voltage of 35 kV on the X-ray tube. The angular step and the exposure time at the angular points were 0.0002° and 1.8 s, respectively.

The angular dependences $I(\Psi)$ of the intensity of refracted radiation on the deflection angle before and after the introduction of a bromonaphthalene sample ($C_{10}H_7Br$) are shown in Fig. 2 (curves *1* and *2*, respectively). The deflection angle Ψ is measured counterclockwise from the axis of the primary beam. Curves *1* and *2* were obtained for the glancing angle $\theta = 0.218°$ between the primary beam and the prism refracting face.

The intense lines in the spectra correspond to the copper anode characteristic emission CuK_α (8.05 keV) and CuK_β (8.90 keV). A well-defined absorption feature appears in the angular spectrum upon the passage of radiation through the bromonaphthalene sample. To simplify its location, it is convenient to use the derivative of the angular spectrum $I(\Psi)$ (curve *3*).

By using the expression for the refractivity decrement [4] and the small-angle approximation for Snell's law, we obtain the relationship

$$E_K = E_0\sqrt{\frac{2\delta_0}{(\Psi_K^2 + 2\theta\Psi_K)}}, \qquad (1)$$

where Ψ_K is the experimentally measured angular position of the K jump in the $I(\Psi)$ curve and E_0 and δ_0 are the energy and refractivity decrement, respectively, of the reference line. The energies of the characteristic CuK_α and CuK_β lines emitted by the tube copper anode can be taken as reference points. Let us consider a multicomponent sample containing m chemical elements. The expression for the relative change in the signal intensity before and after absorption at energies higher (E^+) and lower (E^-) than the given absorption jump edge can be written in the form of the products of exponentials

$$\frac{I(E_{K^-})}{I_0(E_{K^-})} = \exp[-\mu(E_{K^-})\rho L]\exp\left[-\sum_{j=1}^{m-1}\mu_j(E_{K^-})\rho_j L\right], \qquad (2)$$

$$\frac{I(E_{K^+})}{I_0(E_{K^+})} = \exp[-\mu(E_{K^+})\rho L]\exp\left[-\sum_{j=1}^{m-1}\mu_j(E_{K^+})\rho_j L\right], \qquad (3)$$

where $I_0(E_{K^+})$, $I_0(E_{K^-})$ and $I(E_{K^+})$, $I(E_{K^-})$ are the intensities in the spectra of the direct and absorbed beams at energies E_{K^+} and E_{K^-} measured before and after the introduction of the sample, respectively; μ and ρ are the mass attenuation coefficient and the partial density, respectively, of the element whose energy at the absorption jump edge is equal to E_K; μ_j and ρ_j are the partial mass attenuation coefficients and densities of other elements in the sample; and L is the sample size along the direct beam. It is known that, far from the absorption jump, $\mu(E)$ is a smooth and monotonically decreasing function. For this reason, the ratio of the exponential factors containing the summation sign tends to unity at $E_{K^+} \longrightarrow E_K$ and $E_{K^-} \longrightarrow E_K$. The function $\mu(E)$ changes jumpwise in the E_K region. Then, taking the logarithm of Eqs. (2) and (3) and dividing their left- and right-hand sides, one gets

$$\ln\left[\frac{I(E_{K^-})}{I(E_{K^+})}\right] \approx [\mu(E_{K^-}) - \mu(E_{K^+})]\rho L. \qquad (4)$$

If the length L is known, the partial density or the weight content of the element of interest can be determined from Eq. (4); for the known cross-sectional area of the direct beam, the partial mass of the element in the irradiated volume can be found.

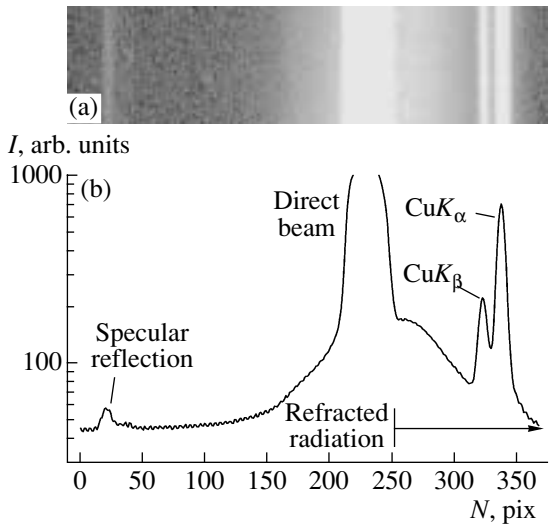

Fig. 3. (a) Two-dimensional image of the refracted X-ray beam pattern. (b) Dependence of the signal intensity on the pixel number for the image in Fig. 3a: (left) peak of specular reflection from the refracting face (N = 23); (center) direct beam (N = 210–250); and (right) bremsstrahlung spectrum (N > 250) and the CuK_β (N = 320) and CuK_α (N = 335) lines.

This is an important advantage of the suggested method over the emission X-ray fluorescence analysis, which when used requires the introduction of complicated corrections.

In conclusion, we present a two-dimensional image of the refraction pattern obtained for the direct beam at a distance of 255 mm from the diamond prism (Fig. 3a). An FDI X-ray camera (Photonic Science) with a two-dimensional array containing 1300 × 1030 pixels was used as a radiation receiver. A Gd oxysulfide layer served as a scintillator. The pixel size was 6.7 μm, and the exposure time was 1 s. Since the photons with different energies are spatially separated after passing through the prism, the spectrum measurement time is of no importance. The radiation flux P through the spectrometer entrance aperture is the only important parameter, because it provides the acceptable signal-to-noise ratio for the image. The dependence of the signal intensity on the pixel number in the central row of the detecting array is shown in Fig. 3b. The integrated refracted-radiation flux P_0 detected at the right side of the image in Fig. 3a was equal to ~10^6 quantum/s. This signifies that, at $P \geq P_0$, the X-ray pulse spectra can be detected by a prism spectrometer without any restrictions on the pulse duration.

This work was supported by the Russian Foundation for Basic Research, project no. 03-02-16976.

REFERENCES

1. A. G. Tur'yanskiĭ, I. V. Pirshin, and R. A. Khmel'nitskiĭ, Kratk. Soobshch. Fiz. **4**, 40 (2000).
2. A. G. Tur'yanskiĭ, I. V. Pirshin, R. A. Khmel'nitskiĭ, *et al.*, Fiz. Tverd. Tela (St. Petersburg) **43**, 619 (2001) [Phys. Solid State **43**, 644 (2001)].
3. A. G. Tur'yanskiĭ, I. V. Pirshin, R. A. Khmel'nitskiĭ, *et al.*, Pis'ma Zh. Éksp. Teor. Fiz. **73**, 517 (2001) [JETP Lett. **73**, 457 (2001)].
4. M. A. Blokhin, *Physics of X-rays* (GITTL, Moscow, 1957).
5. M. A. Blokhin and I. G. Shveĭtser, *X-ray Spectral Handbook* (Nauka, Moscow, 1982).
6. M. Freemantle, *Chemistry in Action* (Macmillan, London, 1987).
7. É. E. Vaĭnshteĭn, *X-ray Spectra of Atoms in Molecules of Chemical Compounds and Alloys* (Akad. Nauk SSSR, Moscow, 1950).

Translated by V. Sakun